^{31}P Chemical Shift of Adsorbed Trialkylphosphine Oxides for Acidity Characterization of Solid Acids Catalysts

Anmin Zheng,[†] Shing-Jong Huang,[‡,§] Wen-Hua Chen,[‡,||] Pei-Hao Wu,[‡] Hailu Zhang,[†] Huang-Kuei Lee,[⊥] Louis-Charles de Ménorval,[#] Feng Deng,*[,†] and Shang-Bin Liu*[,‡]

State Key Laboratory of Magnetic Resonance and Atomic and Molecular Physics, Wuhan Center for Magnetic Resonance, Wuhan Institute of Physics and Mathematics, Chinese Academy of Sciences, Wuhan 430071, China, Institute of Atomic and Molecular Sciences, Academia Sinica, P. O. Box 23-166, Taipei 10617, Taiwan, Institute of Materials Science and Manufacturing, Chinese Culture University, Taipei 11114, Taiwan, and Laboratoire des Agrégats, Interfaces, et Matériaux, pour l'Energie (AIME), Institut Charles Gerhardt Montpellier, UMR-5253 CNRS-UM2-ENSCM-UM1, 34095 Montpellier Cedex 05, France

Received: March 30, 2008; Revised Manuscript Received: June 3, 2008

A comprehensive study has been made to predict the adsorption structures and ^{31}P NMR chemical shifts of various trialkylphosphine oxides (R_3PO) probe molecules, viz., trimethylphosphine oxide (TMPO), triethylphosphine oxide (TEPO), tributylphosphine oxide (TBPO), and trioctylphosphine oxide (TOPO), by density functional theory (DFT) calculations based on 8T zeolite cluster models with varied Si−H bond lengths. A linear correlation between the ^{31}P chemical shifts and proton affinity (PA) was observed for each of the homologous R_3PO probe molecules examined. It is found that the differences in ^{31}P chemical shifts of the R_3POH^+ adsorption complexes, when referring to the corresponding chemical shifts in their crystalline phase, may be used not only in identifying Brønsted acid sites with varied acid strengths but also in correlating the ^{31}P NMR data obtained from various R_3PO probes. Such a chemical shift difference therefore can serve as a quantitative measure during acidity characterization of solid acid catalysts when utilizing ^{31}P NMR of various adsorbed R_3PO, as proposed in our earlier report (Zhao; et al. *J. Phys. Chem. B* **2002**, *106*, 4462) and also illustrated herein by using a mesoporous H-MCM-41 aluminosilicate (Si/Al = 25) test adsorbent. It is indicative that, with the exception of (TMPO), variations in the alkyl chain length of the R_3PO ($R = C_nH_{2n+1}$; $n \geq 2$) probe molecules have only negligible effect on the ^{31}P chemical shifts (within experimental error of ca. 1−2 ppm) either in their crystalline bulk or in their corresponding R_3POH^+ adsorption complexes. Consequently, an average offset of 8 ± 2 ppm was observed for ^{31}P chemical shifts of adsorbed R_3PO with $n \geq 2$ relative to TMPO ($n = 1$). Moreover, by taking the value of 86 ppm predicted for TMPO adsorbed on 8T cluster models as a threshold for superacidity (Zheng; et al. *J. Phys. Chem. B* **2008**, *112*, 4496), a similar threshold ^{31}P chemical shift of ca. 92−94 ppm was deduced for TEPO, TBPO, and TOPO.

1. Introduction

Solid acid catalysts, such as microporous zeolites, mesoporous aluminosilicates, metal oxides, and heteropoly acids, etc., are commonly used during chemical and petrochemical processes.[1–8] Detailed acid properties, namely, the acid type (Brønsted vs Lewis acidity), concentration (amount), strength, and location (intra- vs extracrystalline), are crucial for the catalytic performances (i.e., activity and selectivity) of the solid acid catalysts. A variety of different analytical and spectroscopic techniques, such as titration,[9] calorimetry,[5,10] thermal desorption,[5,11] IR,[12] and NMR,[13–23] have been made available for acidy characterization of solid acid catalysts. Among them, most spectroscopic techniques normally invoke either direct detection of the acidic hydroxyl OH groups or through the adsorption of basic probe molecules containing elements with unpaired electrons (N, O, and P etc.), e.g., ammonia, pyridine, methylamine, or trimethylphosphine (TMP).[12,13]

Nevertheless, while most analytical methods are useful (to various extents) for quantitative determination of the *overall* acidity (acid amount, strength, and distribution), they are incapable of distinguishing the types of acid sites in solid acids.[24] On the other hand, while conventional spectroscopic techniques are more suitable for qualitative characterization (acid type and strength), they are normally inadequate in providing reliable quantitative information of the acid sites.[12–18,22,23] In addition, most experimental acid characterization techniques are handicapped by the difficulty or impossibility of obtaining information on internal and external acid sites, which are essential in understanding the detailed reaction mechanism and related selectivity features of the catalysts.[1,8]

Several novel solid-state NMR techniques have been developed for simultaneous determination of the types and strengths of acid sites in solid acid catalysts, for example, by using ^{13}C magic-angle-spinning (MAS) NMR[22,23] of adsorbed acetone or acetaldehyde or ^{31}P MAS NMR of adsorbed trimethylphosphine (TMP),[14–17] trimethylphosphine oxide (TMPO),[18–20] or triethylphosphine oxide (TEPO)[21] as probes. The advantages of using

* To whom correspondence should be addressed. Fax: +886-2-23620200 (S.-B.L.); +86-27-87199291 (F.D.). E-mail: sbliu@sinica.edu.tw (S.-B.L.); dengf@wipm.ac.cn (F.D.).
[†] Chinese Academy of Sciences.
[‡] Academia Sinica.
[§] Department of Chemistry, National Taiwan University, Taipei 10617, Taiwan.
[||] Present address: Environment and Energy Technology Center, Institute of Nuclear Energy Research, Taoyuan 32546, Taiwan.
[⊥] Chinese Culture University.
[#] UMR-5253 CNRS-UM2-ENSCM-UM1.

10.1021/jp8027319 CCC: $40.75
Published on Web 07/23/2008

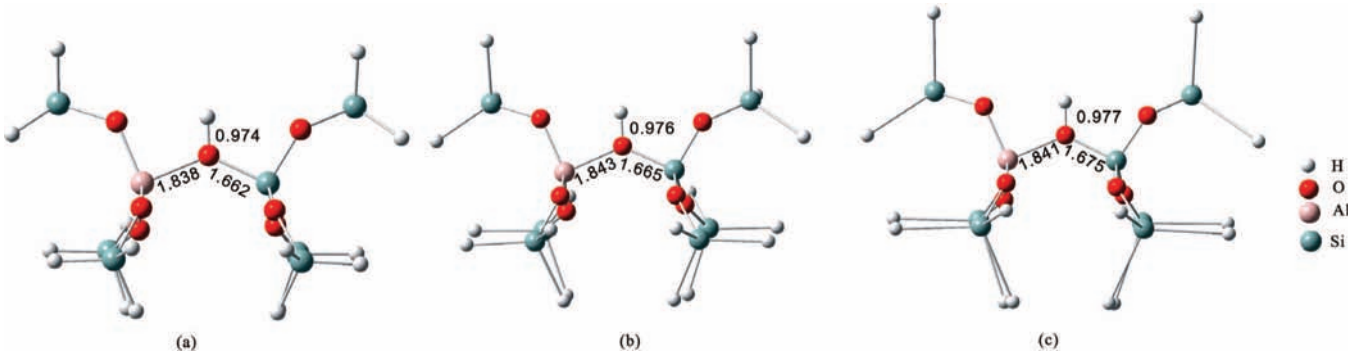

Figure 1. Optimized equilibrium configurations of the 8T zeolite (ZSM-5) cluster model with Si−H bond length (r_{Si-H}) of (a) 1.50, (b) 2.00, and (c) 2.50 Å. Selected interatomic distances (Å) are indicated.

phosphorus molecules over other NMR probes, such as acetone or acetaldehyde, are the higher signal sensitivity and spectral resolution and the wider chemical shift range ($\Delta\delta_r$) possessed by the ^{31}P ($\Delta\delta_r \sim 650$ ppm) nucleus compared to ^{13}C ($\Delta\delta_r \sim 300$ ppm).

By combining elemental analysis with ^{31}P MAS NMR of adsorbed trialkylphosphine oxides (R_3PO) with different molecular sizes, we have demonstrated that detailed acid features, viz., the type, location, concentration, and strength of porous solid acid catalysts, may be determined concurrently.[19,20] In particular, quantitative information on the distribution and concentration of internal vs external acidity can be differentiated by proper choices of R_3PO probe molecules with different sizes.[21] For examples, TMPO and TEPO have kinetic diameters (KDs) of ca. 0.55 and 0.60 nm, respectively, which are smaller than or analogous to the typical pore aperture of 10-membered-ring (10-MR) zeolites (ca. 0.60 nm)[25] and hence are capable of diffusing into the intracrystalline channels/pores of the zeolites, rendering concurrent detection of internal and external acid sites. On the other hand, the sizes of tributylphosphine oxide (TBPO; KD, ca. 0.82 nm) and trioctylphosphine oxide (TOPO; KD, ca. 1.1 nm) are too large to penetrate into the channels/pores of most microporous zeolites and hence can merely detect acid sites located on the extracrystalline surfaces. However, the effect of alkyl-group chain length on the ^{31}P NMR chemical shifts of the R_3PO probe molecules adsorbed on acid sites with varied acidic strengths is still not well understood. This, in turn, makes spectral assignments ambiguous especially in determining the types (Brønsted vs Lewis acidity),[26] strengths and concentrations, and locations (internal vs external acidity) of acid sites based on variations in ^{31}P resonances probed by different R_3PO molecules.

In our previous studies,[19] we proposed to discern internal and external acid sites in a specific porous catalyst (e.g., H-ZSM-5 zeolite) by correlating the respective ^{31}P NMR results obtained from two homologous R_3PO probe molecules (TMPO and TBPO) through the chemical shift differences ($\Delta\delta$) relative to their crystalline bulk. However, theoretical efforts in interpreting the effect of acid strengths on ^{31}P chemical shifts and in correlating the NMR results obtained form different R_3PO probe molecules are still lacking.

Density functional theory (DFT) quantum chemical calculations have been widely used for the predictions of ^{1}H, ^{13}C, and ^{31}P NMR chemical shifts of various probe molecules, such as acetone, pyridine, and TMPO adsorbed on various solid acids, such as zeolites (e.g., MCM-22 and ZSM-5)[23,27–29] and complex oxides (e.g., Mo/ZrO_2 and W/ZrO_2).[30] Recently, we reported the DFT calculations of ^{31}P NMR chemical shifts of adsorbed TMPO and the configurations of the corresponding $TMPOH^+$ complexes on Brønsted acid sites with varied acidic strengths in modeled zeolites.[29] Correlations between the ^{31}P chemical shifts and proton affinity of the solid acids were derived; consequently, a threshold of 86 ppm for ^{31}P chemical shift for TMPO adsorbed on superacid sites in zeolites has been determined.

In this paper, we report the ^{31}P chemical shifts of TMPO, TEPO, TBPO, and TOPO adsorbed on Brønsted acid sites on various porous acid catalysts with varied acidic strengths based on theoretical DFT calculations aiming to explore the effect of R_3PO alkyl chain length on ^{31}P chemical shifts and to validate the discernment of internal vs external acid sites using different R_3PO probes with varied molecular sizes reported earlier.[19] The ^{31}P chemical shifts of adsorbed R_3PO probes so predicted were compared with the experimental results and their correlations with intrinsic acid strengths over a series of microporous zeolites, and mesoporous molecular sieves were also discussed.

2. Experimental Section

2.1. Computational Methods. The acid strength of zeolite can be theoretically simulated by modifying the peripheral Si−H bonds of the cluster model.[31,32] Recently, we have applied this method to explore the correlations of adsorption structures and acid strengths of pyridine and TMPO adsorbed on a series of zeolitic systems[28,29] in which 8T zeolite cluster models, namely, $(H_3SiO)_3-Si-OH-Al-(SiOH_3)_3$, with different terminal Si−H bond lengths were used to represent acid sites with different strengths. Likewise, a similar method can also be used to predict the ^{31}P NMR chemical shifts arising from interactions between various adsorbed R_3PO probe molecules and the bridging hydroxyl (Si−OH−Al) protons of the Brønsted acid sites having varied acid strengths.

Figure 1 shows the assorted 8T cluster models of zeolite ZSM-5 used for DFT calculations in this study. Although more simplified clusters, such as the 3T cluster ($SiH_3-OH-Al(OH)_2-O-SiH_3$) model, have been adopted to interpret acidity in zeolites,[31] the 8T cluster model adopted herein, which has also been used in many earlier studies,[28,29,32] should be more realistic in terms of the effect of zeolite framework on acid site distribution and corresponding adsorption structures.[27] To retain the integrity of the ZSM-5 zeolite structure during the subsequent full optimization of a given 8T cluster, a partial optimization was performed in advance. This was carried out by relaxing the $O_3-Si-OH-Al-O_3$ cluster while keeping the angles of the H_3 groups on the peripheral Si atoms fixed such that they are aligned with the axes connecting Si to the neighboring atoms mimicking the real zeolite structure based on crystallographic data.[33] During the calculations, it was assumed that all of the terminal (Si−H) hydrogen atoms in various clusters are located

at a distance r (Å) from the corresponding silicons with each individual bond orienting along the bond direction to the neighboring oxygen atom. To investigate the correlations between the ^{31}P chemical shifts of adsorbed R_3PO and the Brønsted acid strengths of the solid acid catalyst, a series of different r values (viz., 1.50, 1.75, 2.00, 2.25, 2.50, and 2.75 Å) were used to represent variations in acid strengths (from medium-strong to superacid).[28–32] It is noted that none of the atoms in the adsorbed R_3PO molecules were constrained throughout the configuration optimization processes of the adsorption complexes.

The 8T zeolite clusters and corresponding adsorption structures of R_3PO adsorbed on various Brønsted acid sites (with varied Si−H bond lengths) were optimized with the DMol3 program[34] employing a generalized gradient approximation (GGA)/PW91 density function with DNP basis set[35] (i.e., a double numerical basis function with polarization functions comparable to the Gaussian basis set 6-31G(d,p)).[36] Since neither information on zero point energies nor on thermal corrections were achievable entities in the present study, which involves adsorption of large (R_3PO) molecules on extended (8T) cluster model, they were not accounted for during calculation of adsorption energies even though such correction may be converted to enthalpies that would have been more directly comparable to the experimental results. Subsequently, the ^{31}P NMR chemical shift parameters were calculated using the gauge including atomic orbital (GIAO)[37] approach at MP2/TZVP[38] levels for various R_3POH^+ adsorption complexes on respective 8T cluster models. Using the experimental ^{31}P chemical shift data as benchmarks,[31]P NMR isotropic chemical shifts of the $TMPOH^+$ adsorption complexes were calculated with the MP2 method at the TZVP level and referenced to that of physisorbed TMPO (41 ppm).[18,19] As a result, a corresponding calculated absolute chemical shift value of 346.5 ppm was obtained at the MP2/TZVP level. All the aforementioned NMR parameters were performed by the Gaussian03 package.[39]

2.2. ^{31}P MAS NMR of R_3PO Adsorbed on H-MCM-41. An H-form MCM-41 mesoporous aluminosilicate sample (Si/Al = 25; hereafter denotes as H-MCM-41) with particulate morphology was used as a reference adsorbent in this study. This mesoporous aluminosilicate sample was found to possess an average pore size of 2.57 nm and a BET surface area of ca. 920 m^2/g, as confirmed by N_2 adsorption/desorption isotherm measurements at 77 K. This H-MCM-41 material was chosen as the reference adsorbent mainly due to the fact it has an average pore size that is large enough to accommodate each individual R_3PO adsorbate molecule (viz., TMPO, TEPO, TBPO, and TOPO) whose kinetic diameters range from 0.55 to 1.1 nm,[40] thus facilitating comparison of ^{31}P chemical shifts obtained from various R_3PO probe molecules.

Prior to the adsorption of R_3PO probe molecules, the H-MCM-41 sample was subjected to dehydration treatment at 623 K for 48 h under vacuum (10^{-5} Torr; 1 Torr = 133.32 Pa). Detailed procedures involved in introducing the respective R_3PO probe molecule onto the H-MCM-41 sample can be found elsewhere.[19] In brief, a known amount of R_3PO adsorbate dissolved in anhydrous CH_2Cl_2 was first added into a vessel containing the dehydrated H-MCM-41 sample in a N_2 glovebox, followed by removal of the CH_2Cl_2 solvent by evacuation at 323 K. To ensure a uniform adsorption of adsorbate probe molecules in the pores/channels of the mesoporous adsorbent, the sealed sample vessel was further subjected to a thermal treatment at 483 K for 1 h. Finally, the sample vessel was placed in the N_2 glovebox where the sample was transferred into a

TABLE 1: List of Proton Affinity (PA) and Bridging Hydroxyl Bond Length (r_{Oz-H}) of Bare Cluster and Assorted Bond Distances and Adsorption Energy (ΔE_{ads}) of Various R_3POH^+ Adsorption Complexes Based on 8T Cluster Models with Varied Si−H Bond Lengths (r_{Si-H})

	bare cluster		R_3POH^+ adsorption complex													
			$r_{Oz-H}{}^a$ (Å)				$r_{P=O}{}^b$ (Å)				$r_{O-H}{}^c$ (Å)				adsorption energy (kcal/mol)			
r_{Si-H} (Å)	$r_{Oz-H}{}^a$ (Å)	PA (kcal/mol)	TMPO	TEPO	TBPO	TOPO	TMPO	TEPO	TBPO	TOPO	TMPO	TEPO	TBPO	TOPO	TMPO	TEPO	TBPO	TOPO
1.50	0.974	296.2	1.283	1.308	1.388	1.395	1.549	1.550	1.558	1.559	1.149	1.134	1.089	1.088	23.1	22.6	23.0	23.2
1.75	0.975	282.2	1.399	1.453	1.513	1.497	1.560	1.563	1.571	1.571	1.077	1.063	1.045	1.050	26.6	28.9	29.8	29.1
2.00	0.976	269.2	1.470	1.522	1.581	1.571	1.560	1.571	1.579	1.578	1.056	1.040	1.028	1.032	33.8	35.0	36.3	35.9
2.25	0.977	258.0	1.529	1.615	1.639	1.616	1.568	1.581	1.584	1.585	1.037	1.021	1.017	1.019	37.2	40.6	42.2	42.2
2.50	0.978	249.3	1.602	1.648	1.681	1.666	1.575	1.585	1.590	1.590	1.021	1.013	1.011	41.5	41.5	44.4	45.9	46.4
2.75	0.978	243.7	1.642	1.680	1.710	1.708	1.579	1.588	1.593	1.595	1.014	1.006	1.003	43.6	43.6	48.1	49.4	47.2

[a] r_{Oz-H}: bond length between the acidic proton and zeolite framework oxygen atom. [b] $r_{P=O}$: P=O bond length of the R_3POH^+ ions. [c] r_{O-H}: O−H bond length of the R_3POH^+ ions.

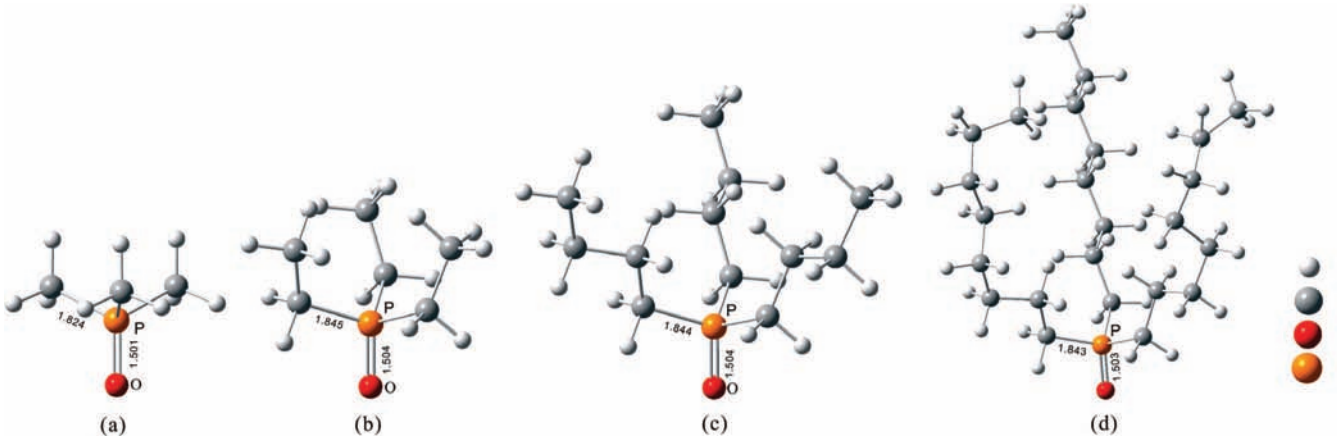

Figure 2. Optimized equilibrium configurations of free (a) TMPO, (b) TEPO, (c) TBPO, and (d) TOPO probe molecules. Selected interatomic distances (Å) are indicated.

ZrO_2 MAS rotor (4 mm o.d.) and then sealed by a gastight Kel-F cap. All ^{31}P MAS NMR experiments were carried out on a Bruker MSL-500P spectrometer operating at a Larmor frequency of 202.46 MHz using a single-pulse sequence with a pulse width of 2 μs (ca. $\pi/5$ pulse), a recycle delay of 10 s, and a typical sample spinning frequency of 12 kHz. Aqueous 85% H_3PO_4 solution was taken as an external reference for the ^{31}P NMR chemical shift.

3. Results and Discussion

3.1. Configurations of R_3PO Adsorbed on Brønsted Acid Sites. As described earlier, the Brønsted acid strengths in zeolites and other porous aluminosilicate catalysts may be theoretically modulated by varying the peripheral Si−H bonds of the 8T cluster model. As illustrated in Figure 1 for a modeled ZSM-5 zeolite, the O−H bond length (r_{Oz-H}) of the bridging hydroxyl groups, which serves as a key parameter to characterize the Brønsted acid strength, increases slightly from 0.974 to 0.978 Å upon increasing the Si−H bond length of the bare cluster from 1.50 to 2.75 Å (Table 1). Nevertheless, discernment of acid strengths based on such small variations in the O−H bond lengths (only ca. 0.004 Å over the whole range of acid strength) alone may be inconclusive. Thus, an alternative indirect method was adopted to characterize the acid strengths. This was done by defining the intrinsic acid strengths as the corresponding proton affinity (PA) values observed for acid sites in solid acid catalysts.[28,29]

The PA value, defined as the energy differences between the protonated (Z−OH) and deprotonated zeolite ($Z-O^-$) models (i.e., PA = $E_{ZOH} - E_{ZO^-}$),[41] represents the extent by which the Brønsted acidic proton is deprotonated. A smaller PA value therefore would reflect greater ease in deprotonating the acid site, and thus a stronger acid strength. As shown in the Table 1, as the Si−H bond distance (r_{Si-H}) of the bare 8T zeolite cluster elongates from 1.50 to 2.75 Å, the corresponding PA values decrease accordingly from 296.2 to 243.7 kcal/mol, covering the typical range of Brønsted acid strengths observed for solid acid catalysts from medium-strong (e.g., in most zeolites) to superacid (e.g., $H_3P_{12}WO_{40}$).[28−32]

The trialkylphosphine oxide (R_3PO) base molecules, which possess partially negative-charged oxygen atoms,[26] tend to interact with the bridging hydroxyl groups (i.e., Brønsted acid sites, which act as proton donors) in zeolites to form hydrogen-bonded R_3POH^+ complexes. Consequently, the density of the electron cloud surrounding the ^{31}P nucleus neighboring to the oxygen atom on a R_3PO probe decreases with increasing acid strength of the Brønsted acid sites, which in turn causes the ^{31}P resonance to shift downfield (i.e., toward a higher chemical shift).[18,19] Furthermore, in view of the fact that the basicity of the four R_3PO probe molecules follow the trend TMPO < TEPO < TBPO ≈ TOPO, which is mainly due to the electronic effect arising from the alkyl groups, it is anticipated that their interatomic bond distances should also be slightly different. Figure 2 displays the optimized equilibrium configurations of various free R_3PO molecules, from which a P═O bond length ($r_{P=O}$) of 1.501, 1.504, 1.504, and 1.503 Å was observed for TMPO, TEPO, TBPO, and TOPO, respectively, whereas the corresponding bond distances between the P atom and the alkyl carbon atom (r_{P-C}) were 1.824, 1.845, 1.844, and 1.843 Å, respectively.

Upon adsorbing the respective R_3PO probe molecule onto various 8T cluster models (with varied r_{Si-H} values), variations in r_{Oz-H} of the bridging hydroxyls as well as the bond distances ($r_{P=O}$ and r_{O-H}) associated with the R_3POH^+ complexes were observed, as depicted in Table 1. As an illustration, the optimized adsorption structures of various systems of various R_3PO probe molecules adsorbed on a specific 8T cluster model with r_{Si-H} = 2.00 Å are shown in Figure 3. By comparing the r_{Oz-H} value (0.976 Å) observed for the bare cluster with r_{Si-H} = 2.00 Å, the values obtained upon adsorption of TMPO, TEPO, TBPO, and TOPO were found to elongate to 1.470, 1.522, 1.581, and 1.571 Å, respectively. By the same token, the $r_{P=O}$ bond distances also elongated to 1.560, 1.571, 1.579, and 1.578 Å, respectively, as compared to their free configuration states (see Figure 2).

As can be seen from Table 1, the bond lengths (r_{O-H}) of the R_3POH^+ complexes, i.e., the distances between the respective R_3PO probe molecules and the proton of the Brønsted acid sites, and the corresponding adsorption energies (ΔE_{ads}) of R_3PO vary not only with acidic strength (i.e., r_{Si-H} or PA) of the cluster models but also with their alkyl chain lengths. Here, we define the ΔE_{ads} values as the energy differences between the absorbed (R_3POH^+-cluster) complex system and the sum of their separated fragments, such that

$$\Delta E_{ads} = (E_{ZOH} + E_{R_3PO}) - E_{R_3PO-ZOH}$$

where $E_{R_3PO-ZOH}$ represents the single-point energy of the optimized $R_{3PO-ZOH}$ complex and E_{ZOH} and $E_{R_3}PO$ are the single-point energies of the optimized bare zeolite cluster (Z−OH) and free R_3PO, respectively. Taking TBPO as an example, for the 8T zeolite cluster with r_{Si-H} = 2.00 Å (PA =

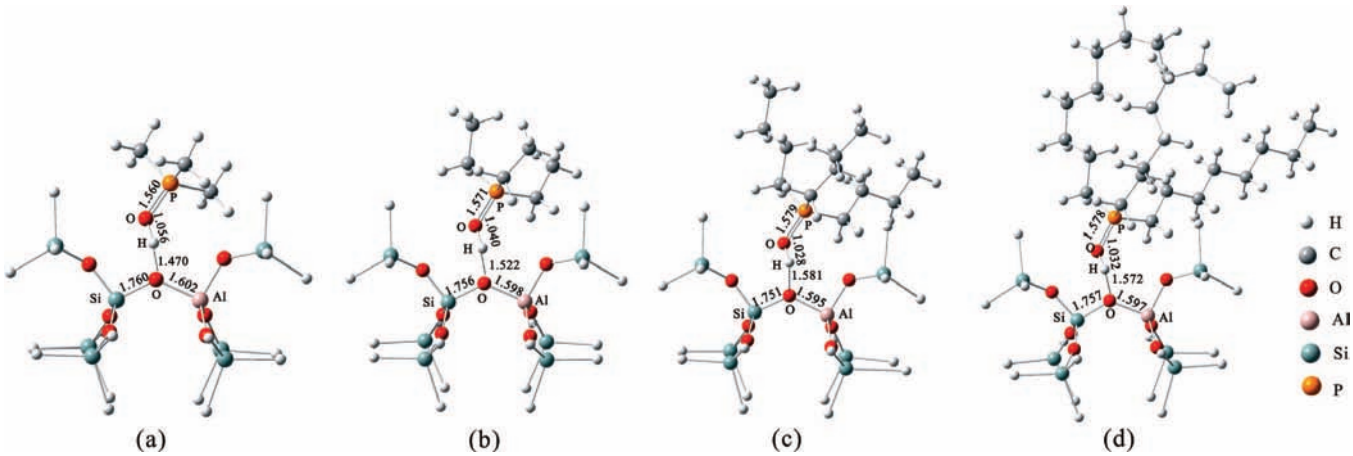

Figure 3. Optimized structures of (a) $TMPOH^+$, (b) $TEPOH^+$, (c) $TBPOH^+$, and (d) $TOPOH^+$ adsorption complexes for an 8T cluster model with Si−H bond length of 2.00 Å. Selected interatomic distances (Å) are indicated.

269.2 kcal/mol; see Table 1), the most obvious change after adsorption of the probe molecule onto the acid catalyst is the elongation of the zeolite−OH bond length (r_{Oz-H}) from 0.976 Å of the bare zeolite cluster to 1.581 Å of the $TBPOH^+$ adsorption complex, leading to a bond distance (r_{O-H}) between the acidic proton and oxygen atom of the TBPO of 1.028 Å (see Figure 3 and Table 1). This clearly indicates the occurrence of the proton being completely transferred from the host adsorbent to the guest adsorbate, forming a $TBPOH^+$ complex. Upon increasing the Brønsted acid strength, e.g., by increasing the r_{Si-H} from 1.50 to 2.75 Å, a gradual decrease in the r_{O-H} value from 1.089 to 1.004 Å was evident. In addition, this phenomenon is also accompanied by the gradual increase in the r_{Oz-H} (from 1.388 to 1.710 Å), $r_{P=O}$ (from 1.558 to 1.593 Å), and ΔE_{ads} (from 23.0 to 49.4 kcal/mol) values of the adsorption complex. Similar conclusions may be drawn for other R_3PO probe molecules (TMPO, TEPO, and TOPO) with varied alkyl chain lengths.

In general, for 8T cluster models with a fixed acid strength (i.e., r_{Si-H} value), gradual increases in the r_{Oz-H}, $r_{P=O}$, and ΔE_{ads} values of the R_3POH^+ adsorption complexes were also observed upon increasing the alkyl chain length of the R_3PO (Table 1). These results are in accordance with the aforementioned trend observed for the basicity of the R_3PO probe molecules. The effects of R_3PO alkyl chain length on the ^{31}P NMR chemical shifts of the R_3POH^+ adsorption complexes will be discussed below.

3.2. Correlations of ^{31}P Chemical Shifts of R_3PO Adsorbed on Brønsted Acid Sites. The calculated ^{31}P NMR chemical shifts of various R_3PO probe molecules adsorbed on Brønsted acid sites of the modeled 8T zeolite cluster with different acid strengths, which were represented in terms of variations in Si−H bond lengths (r_{Si-H}), are depicted in Table 2. For convenience of comparison, the chemical shift differences ($\Delta\delta$) referring to the corresponding chemical shifts with respect to crystalline (bulk) R_3PO are also listed in Table 2. This is made possible by taking the chemical shift values of 39, 48, 47, and 47 ppm for crystalline TMPO, TEPO, TBPO, and TOPO, respectively.[15,17e,18,19] As mentioned earlier, when a given R_3PO probe molecule is adsorbed on a Brønsted acid site that possesses a higher acid strength, as represented by increasing the r_{Si-H} bond length in this study, a notable increase in $r_{P=O}$ can be anticipated (see Table 1). This, in turn, will induce a more negative charge and a greater shielding effect for the P atom, hence leading to a larger ^{31}P chemical shift value. Indeed, such a monotonic increase in the ^{31}P chemical shift with increasing r_{Si-H} (acid strength) was readily observed in the calculation results listed in Table 2 for various R_3PO probes. For example, for TMPO adsorbed on the modeled 8T zeolite cluster, the calculated ^{31}P chemical shift increases from 66.4 to 88.9 ppm while increasing the r_{Si-H} from 1.50 to 2.75 Å, covering the acid strength from medium-strong to superacid. These results are in excellent agreement with the theoretical and experimental data reported earlier,[29] in which a threshold ^{31}P chemical shift of 86 ppm for TMPO was predicted even for much larger (up to 72T) cluster models. Similar observations were found for $TEPOH^+$, $TBPOH^+$, and $TOPOH^+$ adsorption complexes (Table 1).

TABLE 2: ^{31}P Chemical Shifts of Various R_3POH^+ Adsorption Complexes Calculated on the Basis of 8T Cluster Models Having Varied Acid Strengths

		^{31}P chemical shift[a,b] (ppm)			
r_{Si-H} (Å)	PA (kcal/mol)	$TMPOH^+$ ($\Delta\delta$)	$TEPOH^+$ ($\Delta\delta$)	$TBPOH^+$ ($\Delta\delta$)	$TOPOH^+$ ($\Delta\delta$)
1.50	296.2	**66.4** (*27.4*)	**76.2** (*28.2*)	**74.1** (*27.1*)	**75.7** (*28.7*)
1.75	282.2	**74.2** (*35.2*)	**82.2** (*33.2*)	**82.6** (*35.6*)	**81.4** (*34.4*)
2.00	269.2	**76.5** (*37.5*)	**85.2** (*36.2*)	**85.4** (*38.4*)	**85.8** (*38.8*)
2.25	258.0	**81.1** (*42.1*)	**90.8** (*42.8*)	**88.9** (*41.9*)	**89.7** (*42.7*)
2.50	249.7	**85.8** (*46.8*)	**93.5** (*44.5*)	**92.2** (*45.2*)	**92.4** (*45.2*)
2.75	243.7	**88.9** (*49.9*)	**95.7** (*46.7*)	**94.6** (*47.6*)	**95.4** (*48.4*)

[a] GIAO-MP2 calculations normally require more extensive calculation time and disk space compared to the conventional GIAO-HF with the same basis sets; as such, the MP2 method is mostly limited to smaller calculation systems.[27] Thus, the MP2 approximate values were predicted by the equation: $\delta(MP_2,^{31}P) = \delta(MP_2,TMPO) + [\delta(HF,R_3PO) - \delta(HF,TMPO)]$. [b] Data in bold denote theoretical ^{31}P chemical shift values; the italic numbers in parentheses ($\Delta\delta$) refer to the corresponding chemical shift differences with respect to crystalline TMPO (39 ppm), TEPO (48 ppm), TBPO (47 ppm), and TOPO (47 ppm), respectively.

Taking the value of 86 ppm for TMPO adsorbed on the 8T cluster model as the threshold for superacid,[29] which corresponds to an r_{Si-H} value of ca. 2.50 Å and a PA value of ca. 250 kcal/mol, a similar threshold ^{31}P chemical shift of ca. 92−94 ppm was deduced for TEPO, TBPO, and TOPO, respectively, adsorbed on superacid (see Table 2). That these latter three probe molecules have a similar threshold value for superacidity may be attributed to the fact that they have a similar $r_{P=O}$ bond length not only in their crystalline bulk ($r_{P=O} \sim 1.503 \pm 0.001$ Å; see Figure 2) but also in their corresponding adsorption-complex structures ($r_{P=O} \sim 1.588 \pm 0.002$ Å; see Table 1; $r_{Si-H} = 2.50$ Å). As such, it is indicative that, with the exception of

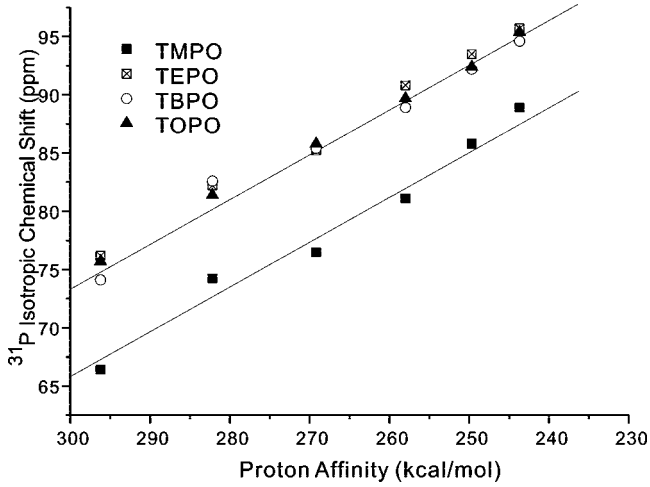

Figure 4. Correlations of calculated ^{31}P chemical shift of adsorbed R_3POH^+ complexes and proton affinity (PA) predicted on the basis of the 8T zeolite cluster models.

trimethylphosphine oxide which contains methyl (CH_3-) groups, variations in the alkyl chain length of the R_3PO (R = C_2H_5-, C_4H_9-, and C_8H_{17}-) probe molecules have only negligible effect on the ^{31}P chemical shifts (within experimental error of ±2 ppm)[19] either in their crystalline bulk or in their corresponding R_3POH^+ adsorption complexes (Table 2). These arguments were further justified experimentally by solid-state ^{31}P MAS NMR of various crystalline R_3PO as well as for various R_3PO adsorbed on a mesoporous Al-MCM-41 molecular sieve (as test catalyst).

The room-temperature ^{31}P MAS spectra of crystalline TMPO, TEPO, TBPO, and TOPO all revealed a single resonance peak at 39, 48, 47, and 47 ppm, respectively (not shown), in good agreement with earlier reports.[14,15,17e,18–21] Again, it is found that the ^{31}P chemical shifts of crystalline TEPO, TBPO, and TOPO all fall in the range of 47−48 ppm, which are about 8−9 ppm downfield compared to that of crystalline TMPO (39 ppm). Moreover, the respective chemical shift differences ($\Delta\delta$) between the adsorbed and crystalline R_3PO predicted by DFT calculations were nearly the same (±2 ppm) for an acid site with a specific acid strength (i.e., the same r_{Si-H} value in Table 2), regardless of the R_3PO alkyl chain length. For example, for modeled zeolite with a moderate acid strength corresponding to r_{Si-H} = 1.50 Å, a close resemblance in the deduced $\Delta\delta$ value (27 ± 1 ppm) was observed for various R_3POH^+ adsorption complexes. However, upon increasing the r_{Si-H} bond length (acid strength) of the modeled cluster from 1.50 (medium-strong) to 2.75 Å (superacid), the averaged $\Delta\delta$ value obtained from various R_3PO complexes increases monotonically from 27 ± 1 to 48 ± 2 ppm. This may readily be seen by plotting the calculated ^{31}P chemical shifts observed for each R_3PO probe molecule against the PA values of the 8T zeolite clusters in Figure 4. Clearly, while the predicted ^{31}P chemical shifts of R_3POH^+ adsorption complexes increase linearly with decreasing PA value (increasing Brønsted acid strength), those observed for TEPO, TBPO, and TOPO nearly coincide with one another at a given PA value, resulting in a nearly constant downfield offset of ca. 8 ± 2 ppm with respect to that observed for TMPO, resembling the aforementioned chemical shift offset (8−9 ppm) among their crystalline bulk.

3.3. Interpretation of ^{31}P Chemical Shifts of R_3PO Adsorbed on H-MCM-41. As explained above, the difference ($\Delta\delta$) between the ^{31}P chemical shifts observed for various R_3POH^+ adsorption complexes and their respective crystalline bulk, which reflects the extent of proton transfer from Brønsted acid sites

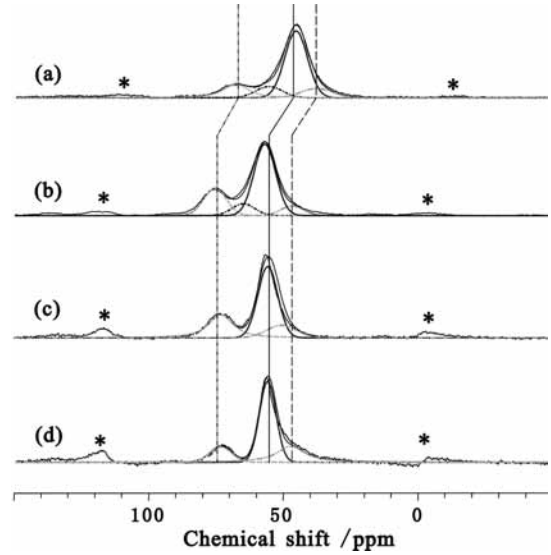

Figure 5. ^{31}P MAS NMR spectra of (a) TMPO, (b) TEPO, (c) TBPO, and (d) TOPO adsorbed on dehydrated H-MCM-41 (Si/Al = 25) catalyst. The dashed curves indicate results of spectral analyses by Gaussian deconvolution. The vertical lines serve as guides to indicate chemical shift offset (8 ± 2 ppm) between the assorted ^{31}P resonances of TMPO and its homologues (TEPO, TBPO, and TOPO). Asterisks (∗) denote spinning sidebands.

TABLE 3: ^{31}P Chemical Shifts of Various R_3PO Adsorbed on the H-MCM-41 (Si/Al = 25) Reference Catalyst

	^{31}P chemical shift[a] (ppm)				
adsorbate	peak 1 ($\Delta\delta$)	peak 2 ($\Delta\delta$)	peak 3 ($\Delta\delta$)	physisorbed	crystalline[b]
TMPO	**68.5** (*29.5*)	**56.7** (*17.7*)	**45.7** (*6.7*)	**40.3**	**39**
TEPO	**75.9** (*27.9*)	**63.6** (*15.6*)	**56.7** (*8.7*)	**47.2**	**48**
TBPO	**73.7** (*26.7*)	-	**56.6** (*9.6*)	**47.1**	**47**
TOPO	**73.7** (*26.7*)	-	**56.2** (*9.2*)	**47.5**	**47**

[a] Data in bold denote experimental ^{31}P chemical shift data; the italic numbers in parentheses ($\Delta\delta$) refer to the corresponding chemical shift differences with respect to their respective crystalline bulk. [b] Data obtained from existing literature.[15,17e,18,19]

to the specified adsorbed R_3PO, may serve as a practical parameter to correlate acid sites with different acid strengths, especially when probe molecules with varied alkyl chain lengths were used. To further justify the feasibility of such correlation method, we have performed ^{31}P MAS NMR measurements to characterize the acid properties of a mesoporous H-MCM-41 aluminosilicate (Si/Al = 25) sample using various R_3PO probe molecules, viz., TMPO, TEPO, TBPO, and TOPO. In this case, the average pore size (2.57 nm) of the reference H-MCM-41 catalyst is much larger than the molecular sizes of the four R_3PO probe molecules, thus rendering adsorption and diffusion of respective adsorbate into the pore channels of the adsorbent.

Figure 5 displays the ^{31}P MAS NMR spectra of various R_3PO adsorbed on H-MCM-41. The results obtained from spectral analysis using the Gaussian deconvolution method (Bruker WINFIT software) are also depicted in Table 3. A total of four resonance peaks can be identified for TMPO adsorbed on H-MCM-41. The resonances at 68.5 and 56.7 ppm can be assigned unambiguously due to TMPO adsorbed on Brønsted acid sites with different acid strengths in the H-MCM-41, whereas the peaks at 45.7 and 40.5 ppm may be attributed to TMPO adsorbed on the silanol groups and physisorbed TMPO, respectively.[19] That the latter peak has a chemical shift resembling that of crystalline TMPO (39 ppm), revealing that the excess TMPO adsorbed in the sample exists as crystalline

bulk. It is noteworthy that no Lewis acidity was found in the H-MCM-41 adsorbent (Si/Al = 25) used in this study; this is consistent with the ^{27}Al MAS NMR results (not shown), which showed the absence of extraframework Al (EFAL) species in the sample.

Similarly, three resonance peaks (at 75.9, 63.6, and 56.7 ppm) were also observed for the $TEPOH^+$ adsorption complexes with varied acidic strengths, while the physisorbed TEPO exhibited a chemical shift at 47.2 ppm, which is also in close proximity with its crystalline bulk (48 ppm; see Table 3). However, it is intriguing that, in addition to their corresponding physisorbed peak (47.1 ppm for TBPO and 47.5 ppm for TOPO), only two ^{31}P resonances were observed for $TBPOH^+$ and $TOPOH^+$ adsorption complexes, respectively. It is hypothesized that the resonances at 56.7 and 63.6 ppm respectively observed by TMPO and TEPO arise from the corresponding $TMPOH^+$ and $TEPOH^+$ adsorption complexes (i.e., probe molecule interacting with Brønsted acid sites) located in the microporous defect of the H-MCM-41. In this context, due to the larger molecular sizes possessed by TBPO and TOPO, they may not penetrate into the microporous defect sites. As such, there are some "hidden" OH groups in the porous acid catalyst that were not readily accessible by these probe molecules, whose sizes exceed the typical pore diameter of microporous zeolites (≤7.5 Å).[19,42] Nevertheless, due to their larger molecular sizes, TBPO and TOPO remain as suitable candidates for probing the external acidity of zeolites.

Further examination of the ^{31}P NMR results obtained from various R_3PO adsorbed on H-MCM-41 (Table 3) reveals that the highest chemical shift values (peak 1), which correspond to acid sites with the highest acid strength in the H-MCM-41 sample, obtained from TMPO, TEPO, TBPO, and TOPO were 68.5, 75.9, 73.7, and 73.7 ppm, respectively. By comparing these experimental values with those calculated on the basis of the 8T cluster model (Table 2), it is indicative that the H-MCM-41 catalyst possesses acid sites with only weak to moderate acid strength, corresponding to a PA value exceeding 296 kcal/mol. Furthermore, the chemical shift differences, $\Delta\delta$, observed from TEPO, TBPO, and TOPO with respect to their respective crystalline bulk are nearly the same (within experimental error of ±2 ppm) and hence should arising from the corresponding probe molecule adsorbed on Brønsted acid sites with similar acid strengths. For example, for acid sites with the highest acid strength (peak 1), a $\Delta\delta$ value of 27.9, 26.7, and 26.7 ppm was observed for $TEPOH^+$, $TBPOH^+$, and $TOPOH^+$ complexes, respectively. Furthermore, a chemical shift offset of ca. 8 ± 2 ppm was observed for TEPO, TBPO, and TOPO relative to that of TMPO, which is in good agreement with our theoretical predictions using the 8T cluster models (see Table 2 and Figure 4).

Similar chemical shift offset was observed for TBPO vs TMPO adsorbed on other porous acid catalysts with a similar Si/Al ratio, such as H-ZSM-5 (Si/Al = 15), H-mordenite (Si/Al = 10), H-USY (Si/Al = 14), H-beta (Si/Al = 12), H-MCM-22 (Si/Al = 13), and H-MCM-41 (Si/Al = 16).[19b] Assorted results obtained from the H-MCM-41 (Si/Al = 25) examined in this study and those from various solid acid catalysts in previous studies[15,18–21] are shown in Figure 6, in which the chemical shift offsets ($\Delta\delta_{TMPO}$) of TEPO, TBPO, and TOPO, respectively relative to TMPO, were plotted against the chemical shifts of TMPO. Regardless of the distribution of acid sites (with varied strengths) in various solid acids, an averaged chemical shift difference of ca. 8 ± 2 ppm can be inferred for the three R_3PO homologous probe molecules (TEPO, TBPO, and TOPO)

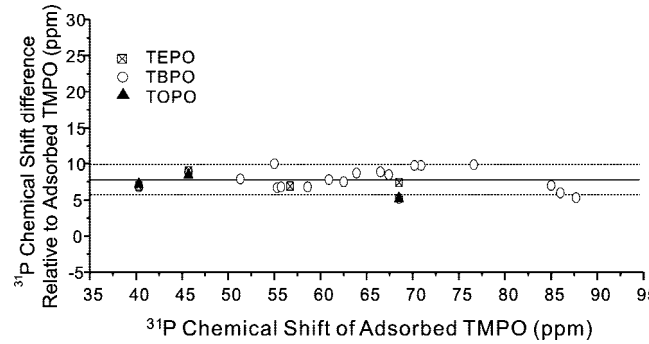

Figure 6. ^{31}P chemical shifts of TEPO, TBPO, and TOPO relative to TMPO adsorbed on various acid catalysts. Collective data were obtained from this study (see Table 3) and existing literature[15,18–21] (see text). The horizontal lines serve as guides for chemical shift offset (8 ± 2 ppm).

relative to TMPO, as indicated by the horizontal dashed line in Figure 6. This observation is in excellent agreement with both the ^{31}P NMR chemical shift offset predicted by DFT calculations based on the 8T zeolite cluster model (Figure 4) as well as that obtained experimentally for various R_3PO adsorbed in H-MCM-41 (Figure 5).

The results obtained from this study therefore afford strong support to the justifiable interpretations of ^{31}P chemical shifts proposed in our previous studies,[19] by which quantitative information on internal and external acidities were obtained by ^{31}P MAS NMR of TMPO and TBPO adsorbed on a variety of different porous solid acid catalysts.

4. Conclusions

The DFT calculations based on a modeled 8T zeolite cluster model in this study revealed that the ^{31}P NMR chemical shifts of various adsorbed trialkylphosphine oxides (R_3PO) adsorbed on solid acid catalysts exhibit a linear correlation with the proton affinity (PA), which was used as a measure of Brønsted acid strength. Accordingly, an averaged downfield offset of ca. 8 ± 2 ppm was found between the ^{31}P chemical shifts of adsorbed TEPO, TBPO, and TOPO relative to that observed for TMPO. As illustrated by experimental ^{31}P MAS NMR measurements of various R_3PO adsorbed on a H-MCM-41 reference catalyst, we have also demonstrated that the difference ($\Delta\delta$) between the ^{31}P chemical shifts observed for an individual R_3PO probe molecule adsorbed on an acid catalyst and its corresponding crystalline bulk may be utilized to identify acid sites having varied acidic strengths when homologous probe molecules with different molecular sizes were used.

The combined theoretical and experimental study reported herein therefore provides not only a theoretical basis but also practical applications in using trialkylphosphine oxides as probe molecules for acidity characterization of solid acid catalysts by solid-state ^{31}P NMR spectroscopy, especially in discerning internal and external acid sites using R_3PO probes with different molecular sizes.

Acknowledgment. This work was supported by the National Natural Science Foundation of China (Grants 20703058, 20773159, 20425311, and 20673139) and by the National Science Council (Grant NSC95-2113-M-001-040-MY3), Taiwan. The authors are grateful to the National Center for High-Performance Computing (NCHC, Taiwan) and Shanghai Supercomputer Center (SSC, China) for their support in computing facilities. A.Z. thanks NSC and IAMS, Academia Sinica, for the visiting research fellowship, and S.-B.L. is grateful for the

visiting professorship from Institut Charles Gerhardt Montpellier, Laboratoire des Agrégats, Interfaces et Matériaux pour L'Energie (ICG-AIME-UMR 5253), CNRS, Montpellier, France.

References and Notes

(1) Chen, N. Y.; Degnan, T. F.; Smith, C. M. *Molecular Transport and Reaction in Zeolites: Design and Application of Shape Selective Catalysts*; VCH: New York, 1994.

(2) Souverijns, W.; Verrelst, W.; Vanbutsele, G.; Martens, J. A.; Jacobs, P. A. *J. Chem. Soc., Chem. Commun.* **1994**, 1671.

(3) (a) Corma, A. *Chem. Rev.* **1995**, *95*, 559. (b) Corma, A.; Martinez-Triguero, J. *J. Catal.* **1997**, *165*, 102.

(4) Guisnet, M. *Acc. Chem. Res.* **1990**, *23*, 392.

(5) (a) Chronister, C. W.; Drago, R. S. *J. Am. Chem. Soc.* **1993**, *115*, 793. (b) Drago, R. S.; Dias, S. C.; Torrealba, M.; de Lima, L. *J. Am. Chem. Soc.* **1997**, *119*, 4444.

(6) (a) Verhoef, M. J.; Creyghton, E. J.; Peters, J. A. *Chem. Commun. (Cambridge)* **1997**, 1989. (b) Wu, P.; Takayuki, K.; Tatsuaki, Y. *Microporous Mesoporous Mater.* **1998**, *22*, 343.

(7) (a) Barthos, R.; Lonyi, F.; Onyestyak, G.; Valyon, J. *J. Phys. Chem. B* **2000**, *104*, 7311. (b) Tessonnier, J. P.; Louis, B.; Walspurger, S.; Sommer, J.; Ledoux, M.; Pham-Huu, C. *J. Phys. Chem. B.* **2006**, *110*, 10390.

(8) (a) Tsai, T. C.; Liu, S. B.; Wang, I. *Appl. Catal., A* **1999**, *181*, 355. (b) Chen, W. H.; Tsai, T. C.; Jong, S. J.; Zhao, Q.; Tsai, C. T.; Lee, H. K.; Wang, I.; Liu, S. B. *J. Mol. Catal. A* **2002**, *181*, 41.

(9) Moscou, L.; Moné, R. *J. Catal.* **1973**, *30*, 417.

(10) (a) Védrine, J. C.; Auroux, A.; Bolis, V.; Dejaifve, P.; Naccache, C.; Wierzchowski, P.; Derouane, E. G.; Nagy, J. B.; Gilson, J. P.; van Hooff, J. H. C.; van den Berg, J. P.; Wolthuizen, J. *J. Catal.* **1979**, *59*, 248. (b) Kapustin, G. I.; Brueva, T. R.; Klyachko, A. L.; Beran, S.; Wichterlová, B. *Appl. Catal.* **1988**, *42*, 239.

(11) (a) Topsøe, N Y.; Pedersen, K.; Derouane, E. G. *J. Catal.* **1981**, *70*, 41. (b) Jacobs, P. A.; Martens, J. A.; Weitkamp, J.; Beyer, H. K. *Faraday Discuss. Chem. Soc.* **1981**, *72*, 353. (c) Narayanan, S.; Sultana, A.; Thinh Le, Q.; Auroux, A. *Appl. Catal., A* **1998**, *168*, 373.

(12) (a) Lercher, J. A.; Gründling, C.; Eder-Mirth, G. *Catal. Today* **1996**, *27*, 353. (b) Kustov, L. M. *Top. Catal.* **1997**, *4*, 131.

(13) (a) Pfeifer, H.; Freude, D.; Hunger, M. *Zeolites* **1985**, *5*, 274. (b) Hunger, M. *Catal. Rev.−Sci. Eng.* **1997**, *39*, 345.

(14) (a) Maciel, G. E.; Ellis, P. D. In *NMR Techniques in Catalysis*; Bell, A. T., Pines, A. Eds.; Dekker: New York, 1994; pp 231−309.

(15) (a) Baltusis, L.; Frye, J. S.; Maciel, G. E. *J. Am. Chem. Soc.* **1986**, *108*, 7119. (b) Baltusis, L.; Frye, J. S.; Maciel, G. E. *J. Am. Chem. Soc.* **1987**, *109*, 40.

(16) (a) Lunsford, J. H.; Rothwell, W. P.; Shen, W. *J. Am. Chem. Soc.* **1985**, *107*, 1540. (b) Lunsford, J. H. *Top. Catal.* **1997**, *4*, 91. (c) Zhao, B.; Pan, H.; Lunsford, J. H. *Langmuir* **1999**, *15*, 2761. (d) Hu, B.; Gay, I. D. *Langmuir* **1999**, *15*, 477. (e) Haw, J. F.; Zhang, J. H.; Shimizu, K.; Venkatraman, T. N.; Luigi, D. P.; Song, W. G.; Barich, D. H.; Nicholas, J. B. *J. Am. Chem. Soc.* **2000**, *122*, 12561.

(17) (a) Grey, C. P.; Veeman, W. S.; Vega, A. J. *J. Chem. Phys.* **1993**, *98*, 7711. (b) Grey, C. P.; Vega, A. J. *J. Am. Chem. Soc.* **1995**, *117*, 8232. (c) Kao, H. M.; Grey, C. P. *Chem. Phys. Lett.* **1996**, *259*, 459. (d) Kao, H. M.; Liu, H. M.; Jiang, J. C.; Lin, S. H.; Grey, C. P. *J. Phys. Chem. B* **2000**, *104*, 4923. (e) Kao, H. M.; Yu, C. Y.; Yeh, M. C. *Microporous Mesoporous Mater.* **2002**, *53*, 1.

(18) (a) Rakiewicz, E. F.; Peters, A. W.; Wormsbecher, R. F.; Sutovich, K. J.; Mueller, K. T. *J. Phys. Chem. B* **1998**, *102*, 2890. (b) Karra, M. D.; Sutovich, K. J.; Mueller, K. T. *J. Am. Chem. Soc.* **2002**, *124*, 902. (c) Osegovic, J. P.; Drago, R. S. *J. Catal.* **1999**, *182*, 1. (d) Osegovic, J. P.; Drago, R. S. *J. Phys. Chem. B* **2000**, *104*, 147.

(19) (a) Zhao, Q.; Chen, W. H.; Huang, S. J.; Wu, Y. C.; Lee, H. K.; Liu, S. B. *J. Phys. Chem. B* **2002**, *106*, 4462, and references threin. (b) Zhao, Q.; Chen, W. H.; Huang, S. J.; Liu, S. B. *Stud. Surf. Sci. Catal.* **2003**, *145*, 205.

(20) (a) Chen, W. H.; Ko, H. H.; Sakthivel, A.; Huang, S. J.; Liu, S. H.; Lo, A. Y.; Tsai, T. C.; Liu, S. B. *Catal. Today* **2006**, *116*, 111. (b) Huang, S. J.; Tseng, Y. H.; Mou, Y.; Liu, S. B.; Huang, S. H.; Lin, C. P.; Chan, J. C. C. *Solid State Nucl. Magn. Reson.* **2006**, *29*, 272. (c) Alonso, B.; Klur, I.; Massiot, D. *Chem. Commun. (Cambridge)* **2002**, 804.

(21) Margolese, D.; Melero, J. A.; Christiansen, S. C.; Chmelka, B. F.; Stucky, G. D. *Chem. Mater.* **2000**, *12*, 2448.

(22) (a) Biaglow, A. I.; Šepa, J.; Gorte, R. J.; White, D. *J. Catal.* **1995**, *151*, 373. (b) Fărcaşiu, D.; Ghenciu, A. *Prog. Nucl. Magn. Reson. Spectrosc.* **1996**, *29*, 129.

(23) Zheng, A.; Chen, L.; Yang, J.; Zhang, M.; Su, Y.; Yue, Y.; Ye, C.; Deng, F. *J. Phys. Chem. B* **2005**, *109*, 24273.

(24) (a) Van Hooff, J. H. C.; Roelofsen, J. W. *Stud. Surf. Sci. Catal.* **1991**, *58*, 241. (b) Gruver, V.; Panov, A.; Fripiat, J. J. *Langmuir* **1996**, *12*, 2505.

(25) Breck, D. W. In *Zeolite Molecular Sieves: Structure, Chemistry, and Use*; John Wiley & Sons: New York, 1974.

(26) Engelhardt, L. M.; Raston, C. L.; Whitaker, C. R.; White, A. H.; Aust, *J. Chem.* **1986**, *39*, 2151.

(27) (a) Xu, T.; Torres, P. D.; Barich, D. H.; Nicholas, J. B.; Haw, J. F. *J. Am. Chem. Soc.* **1997**, *119*, 396. (b) Xu, T.; Barich, D. H.; Torres, P. D.; Haw, J. F. *J. Am. Chem. Soc.* **1997**, *119*, 406.

(28) (a) Zheng, A.; Chen, L.; Yang, J.; Yue, Y.; Ye, C.; Lu, X.; Deng, F. *Chem. Commun. (Cambridge)* **2005**, 2474. (b) Zheng, A.; Zhang, H. L.; Chen, L.; Yue, Y.; Ye, C.; Deng, F. *J. Phys. Chem. B* **2007**, *111*, 3085.

(29) Zheng, A.; Zhang, H. L.; Lu, X.; Liu, S. B.; Deng, F. *J. Phys. Chem. B* **2008**, *112*, 4496.

(30) Xu, J.; Zheng, A.; Yang, J.; Su, Y.; Wang, J.; Zeng, D.; Zhang, M.; Ye, C.; Deng, F. *J. Phys. Chem. B* **2006**, *110*, 10662.

(31) Kramer, G. J.; van Santen, R. A.; Emeis, C. A.; Nowak, A. K. *Nature* **1993**, *363*, 529.

(32) Zheng, X.; Blowers, P. *J. Mol Catal. A* **2005**, *229*, 77. (b) Zheng, X.; Blowers, P. *J. Phys. Chem. A* **2005**, *109*, 10734.

(33) van Koningsveld, H.; van Bekkum, H.; Jansen, J. C. *Acta Crystallogr., B* **1987**, *43*, 127.

(34) *DMo13*; Accelrys: San Diego, CA, 2006.

(35) Perdew, J. P.; Wang, Y. *Phys. Rev. B* **1986**, *33*, 8822.

(36) Hehre, W. J.; Ditchfield, J. A.; Pople, J. A. *J. Chem. Phys.* **1972**, *56*, 2257.

(37) (a) Ditchfield, R. *Mol. Phys.* **1974**, *27*, 789. (b) Wolinski, K.; Hinton, J. F.; Pulay, P. *J. Am. Chem. Soc.* **1990**, *112*, 8251.

(38) Godbout, N.; Salahub, D. R.; Andzelm, J.; Wimmer, E. *Can. J. Chem.* **1992**, *70*, 560.

(39) Frisch, M. J.; Trucks, G. W.; Schlegel, H. B.; Scuseria, G. E.; Robb, M. A.; Cheeseman, J. R.; Montgomery, J. A., Jr.; Vreven, T.; Kudin, K. N.; Burant, J. C.; Millam, J. M.; Lyengar, S. S.; Tomasi, J.; Barone, V.; Mennucci, B.; Cossi, M.; Scalmani, G.; Rega, N.; Petersson, G. A.; Nakatsuji, H.; Hada, M.; Ehara, M.; Toyota, K.; Fukuda, R.; Hasegawa, J.; Ishida, M.; Nakajima, T.; Honda, Y. ; Kitao,O.; Nakai, H.; Klene, M.; Li, X.; Knox, J. E.; Hratchian, H. P.; Cross, J. B.; Adamo, C.; Jaramillo, J.; Gomperts, R.; Stratmann, R. E.; Yazyev, O.; Austin, A. J.; Camml, R.; Pomelli, C.; Ochterski, J. W.; Ayala, P. Y.; Morokuma, K.; Voth, G. A.; Salvador, P.; Dannenberg, J. J.; Zakrzewski, V. G.; Dapprich, S.; Daniels, A. D.; Strain, M. C.; Farkas, O.; Malick, D. K.; Rabuck, A. D.; Raghavachari, K.; Foresman, J. B.; Ortiz, J. V.; Cui, Q.; Baboul, A. G.; Clifford, S.; Cioslowski, J.; Stefanov, B. B.; Liu, G.; Liashenko, A.; Piskorz, P.; Komaromi, I.; Martin, R. L.; Fox, D. J.; Keith, T.; Al-Laham, M. A.; Peng, C. Y.; Nanayakkara, A.; Challacombe, M.; Gill, P. M. W.; Johnson, B.; Chen, W.; Wong, M. W.; Gonzalez, C.; Pople, J. A. *Gaussian 03*, Revision B.05; Gaussian: Pittsburgh, PA, 2003.

(40) Based on the optimized configurations of free R_3PO, the molecular size of TMPO, TEPO, TBPO, and TOPO were estimated to be 0.47, 0.54, 0.86, and 1.16 Å, respectively.

(41) Nicholas, J. B. *Top. Catal.* **1999**, *9*, 181.

(42) Shenderovich, I. G.; Buntkowsky, G.; Schreiber, A.; Gedat, E.; Sharif, S.; Albrecht, J.; Golubev, N. S.; Findenegg, G. H.; Limbach, H. *J. Phys. Chem. B* **2003**, *107*, 11924.

JP8027319